# Spectral and Energy Efficient User Pairing for RIS-assisted Uplink NOMA Systems with Imperfect Phase Compensation

Kusuma Priya P., Pavan Reddy M., Abhinav Kumar

Department of Electrical Engineering, Indian Institute of Technology Hyderabad, India 502285

Email:{ee20mtech11007, ee14resch11005}@iith.ac.in, abhinavkumar@ee.iith.ac.in

*Abstract*—Non-orthogonal multiple access (NOMA) is considered a key technology for improving the spectral efficiency of fifth-generation (5G) and beyond 5G cellular networks. NOMA is beneficial when the channel vectors of the users are in the same direction, which is not always possible in conventional wireless systems. With the help of a reconfigurable intelligent surface (RIS), the base station can control the directions of the channel vectors of the users. Thus, by combining both technologies, the RIS-assisted NOMA systems are expected to achieve greater improvements in the network throughput. However, ideal phase control at the RIS is unrealizable in practice because of the imperfections in the channel estimations and the hardware limitations. This imperfection in phase control can have a significant impact on the system performance. Motivated by this, in this paper, we consider an RIS-assisted uplink NOMA system in the presence of imperfect phase compensation. We formulate the criterion for pairing the users that achieves minimum required data rates. We propose adaptive user pairing algorithms that maximize spectral or energy efficiency. We then derive various bounds on power allocation factors for the paired users. Through extensive simulation results, we show that the proposed algorithms significantly outperform the state-of-the-art algorithms in terms of spectral and energy efficiency.

*Index Terms*—Energy efficiency, non-orthogonal multiple access, power allocation, reconfigurable intelligent surface, spectral efficiency, uplink, user pairing.

## I. INTRODUCTION

In the fifth-generation (5G) and beyond 5G communication systems, significant improvements are expected in terms of spectral efficiency, energy conservation, massive connectivity, and latency requirements. Non-orthogonal multiple access (NOMA) is considered as a key multiple access technique to enhance the spectral efficiency of future cellular networks [1]. Various NOMA transmission schemes have been evaluated for possible consideration of NOMA in 5G uplink scenario [2]. In NOMA, multiple users are allocated with the same time and frequency resources to achieve multi-fold improvement in the network throughputs. However, the users are multiplexed in either power domain (power-domain NOMA) or code domain (code-domain NOMA), which requires the receiver to employ a successive interference cancellation (SIC) and decode the data [3]. Similar to NOMA, reconfigurable intelligent surface (RIS) is considered as a key technology to improve the spectral efficiency of the cellular networks [4]. An RIS is a two-dimensional planar array consisting of low-cost reflecting antenna elements that can modify the amplitude and phase of the signal. Thus, by using RIS, the base station (BS) can perform beamforming and transmit the signal in the desired direction.

Unlike the spatial multiplexing in orthogonal multiple access (OMA), NOMA is beneficial in situations where the channel vectors of users are in the same direction [4]. This is not always possible in conventional wireless systems, whereas, in the case of RIS-assisted systems, the BS can control the direction of the user channel vectors by tuning the RIS [4], [5]. For these reasons, RIS-assisted NOMA systems have been widely considered to achieve significant improvements in the network performance [4], [6]. However, the ideal phase control is difficult to achieve in practice for various reasons like hardware impairments, channel estimation errors, etc. These imperfections in the phase control degrade the achievable spectral and energy efficiencies in the network. Further, in NOMA systems, the achievable data rates are significantly dependent on the user pairing, and hence, while pairing the users in RIS-assisted NOMA systems, the network operator has to consider the imperfections in the phase compensation. Otherwise, the expected improvements in the network throughputs will not be realized in practice. For the aforementioned reasons, investigating the effect of imperfection in phase at the RIS is crucial to achieve optimum system performance.

In [7], [8], the authors have proposed various channel estimation techniques for RIS-assisted wireless systems. In [9], [10], the authors have formulated the sum-rate maximization as an optimization problem, and then, derived a near-optimal solution for RIS-assisted uplink NOMA systems. However, limited works in the literature have considered the imperfection in phase for the downlink OMA and NOMA systems [6], [11], [12]. To the best of our knowledge, none of the existing works considered the imperfections in the phase compensation while pairing the users in RIS-assisted uplink NOMA systems. Motivated by this, we present the following key contributions in this paper.

- For RIS-assisted uplink NOMA systems, we derive bounds on imperfection in the phase compensation to achieve minimum required data rates.
- We propose user pairing algorithms that maximize spectral efficiency and energy efficiency, respectively.
- We derive bounds and define the power allocation factors for the paired users.
- Through extensive simulation results, we show that the proposed algorithms significantly outperform the state-of-the-art algorithms.

The rest of the paper is organized as follows. The system model is presented in Section II. In Section III, we propose the adaptive user pairing algorithms, derive the bounds on the power allocation factors, and formulate the criterion for pairing the users to maximize spectral and energy efficiencies. In Section IV, we present the simulation results for various scenarios. Section V presents some concluding remarks and possible future works.
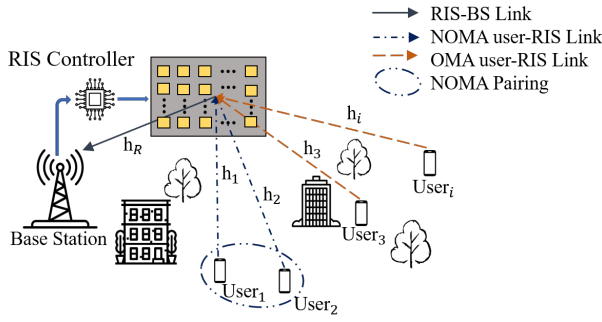
Fig. 1: System model.

## II. SYSTEM MODEL

We consider an uplink scenario with $M$ antennae at the BS, $N$ reflective antenna elements at the RIS, and a single antenna at each user as shown in Fig. 1. The direct link between the BS and user is assumed to be blocked by the obstacles such as buildings, trees, or human body which is a likely scenario in case of mmwave communications [11]. Further, the channel coefficients from $i^{th}$ user to RIS and RIS to BS are defined as $\mathbf{h}_i$ and $\mathbf{h}_R$, respectively and are formulated as follows [11]

$$\mathbf{h}_i = \beta_i \mathbf{a}_N\left(\psi_I^a, \psi_I^e\right), \tag{1}$$
$$\mathbf{h}_R = \alpha \mathbf{a}_N\left(\phi_I^a, \phi_I^e\right)\mathbf{a}_M^H\left(\psi_B^a, \psi_B^e\right), \tag{2}$$

where $\beta_i$ and $\alpha$ denote the channel gains from $i^{th}$ user to RIS and RIS to BS, respectively, $\phi_I^a$ and $\phi_I^e$ represent the angle of departure (AoD) in azimuth and elevation at the RIS, respectively, $\psi_B^a$ and $\psi_B^e$ represent angle of arrival (AoA) in azimuth and elevation at the BS, respectively, $\psi_I^a$ and $\psi_I^e$ represent the AoA in azimuth and elevation at the RIS, respectively, and $\mathbf{a}_X(\Omega^a, \Omega^e)$ represents the array response vector. A uniform square planar array (USPA) with $X$ antenna elements, has $\sqrt{X}$ elements in both horizontal and vertical directions, and thus, the array response vector is defined as

$$\mathbf{a}_X(\Omega^a, \Omega^e) = \begin{bmatrix} 1 \\ \vdots \\ e^{j\frac{2\pi d}{\lambda}(x\sin\Omega^a\sin\Omega^a + y\cos\Omega^e)} \\ \vdots \\ e^{j\frac{2\pi d}{\lambda}((\sqrt{X}-1)(\sin\Omega^a\sin\Omega^a)+(\sqrt{X}-1)\cos\Omega^e)} \end{bmatrix}^T,$$

where, $d$ is the equispaced elemental distance, $\lambda$ is the signal wavelength, $0 \le x, y \le \sqrt{X} - 1$ are the indices of the USPA elements in the horizontal and vertical directions, respectively.

We denote the reflection matrix at the RIS as $\boldsymbol{\Theta}$ and define it as follows [4].

$$\boldsymbol{\Theta} = \mathrm{diag}(e^{j\theta_1}, \ldots, e^{j\theta_k}, \ldots, e^{j\theta_N}),$$

where, $\theta_k$ $(1 \le k \le N)$ is the phase shift introduced by $k^{th}$ reflecting element at the RIS. However, note that the ideal phase control is difficult to achieve in practice because of various reasons like hardware limitations and imperfect channel state information [6], [11], [12]. For this reason, we consider imperfections in the phase control and define the practical reflection matrix as follows.

$$\tilde{\boldsymbol{\Theta}} = \mathrm{diag}(e^{j\tilde{\theta}_1}, \ldots, e^{j\tilde{\theta}_k}, \ldots, e^{j\tilde{\theta}_N}),$$

where, $\tilde{\theta}_k = \theta_k + \hat{\theta}_k$ with $\hat{\theta}_k$ being the error in phase control at $k^{th}$ antenna element. Further, we assume $\hat{\theta}_k$ to be uniformly distributed over $[-\delta, \delta]$, $\delta \in [0, \pi)$. Thus, in the case of OMA transmission, the signal received from the $i^{th}$ user at the BS is formulated as

$$y_i^{\mathrm{OMA}} = \mathbf{h}_R^H \tilde{\boldsymbol{\Theta}} \mathbf{h}_i P_t s_i + n_i,$$

where $\{.\}^{\mathrm{H}}$ denotes the Hermitian of a matrix, $P_t$ is the available transmit power at each user, $s_i$ is the data symbol transmitted by the $i^{th}$ user, and $n_i$ denotes the thermal noise. The signal to interference plus noise ratio (SINR) of an $i^{th}$ user in an RIS-assisted OMA system is formulated as

$$\gamma_i^{\mathrm{OMA}} = \frac{P_t\|\mathbf{h}_R^H \tilde{\boldsymbol{\Theta}} \mathbf{h}_i\|^2}{I + \sigma^2}, \tag{3}$$

where $I$ is the interference power and $\sigma^2$ is the noise variance. In the case of RIS assisted NOMA, we consider two users multiplexed in the power domain, with channel coefficients $\mathbf{h}_1$ and $\mathbf{h}_2$. Additionally, we assume the following

$$\|\mathbf{h}_R^H \tilde{\boldsymbol{\Theta}} \mathbf{h}_1\|^2 > \|\mathbf{h}_R^H \tilde{\boldsymbol{\Theta}} \mathbf{h}_2\|^2.$$

Thus, the BS receives $P_t(\alpha_1 s_1 + \alpha_2 s_2)$, where $s_1$ and $s_2$ are the data symbols transmitted by the strong and weak user, respectively. Further, we consider a fractional power control scenario, where $0 < \alpha_1, \alpha_2 \le 1$ represent the fraction of the total available transmit power used by the strong and weak users, respectively. Thus, the signal received from the $i^{th}$ user in an RIS-assisted NOMA system is formulated as follows

$$y_i^{\mathrm{NOMA}} = \mathbf{h}_R^H \tilde{\boldsymbol{\Theta}} \mathbf{h}_i P_t(\alpha_1 s_1 + \alpha_2 s_2) + n_i. \tag{4}$$

From (4), we define the SINR of the users in RIS-assisted NOMA as follows

$$\gamma_1^{\mathrm{NOMA}} = \frac{\alpha_1 P_t\|\mathbf{h}_R^H \tilde{\boldsymbol{\Theta}} \mathbf{h}_1\|^2}{\alpha_2 P_t\|\mathbf{h}_R^H \tilde{\boldsymbol{\Theta}} \mathbf{h}_2\|^2 + I + \sigma^2}, \tag{5}$$

$$\gamma_2^{\mathrm{NOMA}} = \frac{\alpha_2 P_t\|\mathbf{h}_R^H \tilde{\boldsymbol{\Theta}} \mathbf{h}_2\|^2}{I + \sigma^2}. \tag{6}$$

From (1)-(2), we define the following [6]:

$$\mathbf{h}_R^H \tilde{\boldsymbol{\Theta}} \mathbf{h}_i = \alpha\beta_i \mathbf{a}_M(\psi_B^a, \psi_B^e)\sum_{k=1}^{N} e^{j\hat{\theta}_k},$$

$$\|\mathbf{a}_M(\psi_B^a, \psi_B^e)\|^2 = M,$$

$$\|\mathbf{h}_R^H \tilde{\boldsymbol{\Theta}} \mathbf{h}_i\|^2 = |\alpha\beta_i|^2 M\left|\sum_{k=1}^{N} e^{j\hat{\theta}_k}\right|^2. \tag{7}$$

We adopt the following approximation from [11]:

$$\left|\frac{1}{N}\sum_{k=1}^{N} e^{j\hat{\theta}_k}\right|^2 \xrightarrow{(a)} \left|\mathbb{E}\left[e^{j\hat{\theta}_k}\right]\right|^2 \stackrel{(b)}{=} \left|\mathbb{E}\left[\cos\hat{\theta}_k\right]\right|^2 \stackrel{(c)}{=} \mathrm{sinc}^2(\delta), \tag{8}$$

where $(a)$ follows the strong law of large numbers [11], in $(b)$, the expectation of odd function $\sin\hat{\theta}_k$ vanishes over the interval $\hat{\theta}_k \in [-\delta, \delta]$, and $(c)$ is obtained by using the probability density function $f(\hat{\theta}_k) = \frac{1}{2\delta}$, where $\hat{\theta}_k \in [-\delta, \delta]$.

Substituting (8) in (7)

$$\|\mathbf{h}_R^H \tilde{\boldsymbol{\Theta}} \mathbf{h}_i\|^2 = |\alpha\beta_i|^2 MN^2 \operatorname{sinc}^2(\delta),$$
$$\|\mathbf{h}_R^H \boldsymbol{\Theta} \mathbf{h}_i\|^2 = |\alpha\beta_i|^2 MN^2.$$

Using these approximations, we define the channel state information (CSI) of $i^{th}$ user as

$$\gamma_i^{\text{CSI}} \triangleq \frac{P_t \|\mathbf{h}_R^H \boldsymbol{\Theta} \mathbf{h}_i\|^2}{I + \sigma^2} = \frac{P_t |\alpha\beta_i|^2 N^2 M}{I + \sigma^2}. \tag{9}$$

Using (9) in (3), (5), and (6), we formulate the received SINRs as follows

$$\gamma_i^{\text{OMA}} = \gamma_i^{\text{CSI}} \operatorname{sinc}^2(\delta),$$
$$\gamma_1^{\text{NOMA}} = \frac{\alpha_1 \gamma_1^{\text{CSI}} \operatorname{sinc}^2(\delta)}{1 + \alpha_2 \gamma_2^{\text{CSI}} \operatorname{sinc}^2(\delta)},$$
$$\gamma_2^{\text{NOMA}} = \alpha_2 \gamma_2^{\text{CSI}} \operatorname{sinc}^2(\delta).$$

Given a logarithmic rate model, the normalized achievable data rates by the users in OMA and NOMA are formulated as [12]

$$R_i^{\text{OMA}} = \frac{1}{2} \log_2 \left( 1 + \gamma_i^{\text{CSI}} \operatorname{sinc}^2(\delta) \right), \tag{10}$$

$$R_1^{\text{NOMA}} = \log_2 \left( 1 + \frac{\alpha_1 \gamma_1^{\text{CSI}} \operatorname{sinc}^2(\delta)}{1 + \alpha_2 \gamma_2^{\text{CSI}} \operatorname{sinc}^2(\delta)} \right), \tag{11}$$

$$R_2^{\text{NOMA}} = \log_2 \left( 1 + \alpha_2 \gamma_2^{\text{CSI}} \operatorname{sinc}^2(\delta) \right). \tag{12}$$

Next, we propose various adaptive user pairing algorithms.

## III. Proposed Algorithms

In this section, we propose maximum ASR power allocation (MPA) and energy efficient power allocation (EEPA) algorithms to maximize the sum rate and energy efficiency, respectively. Additionally, in both the algorithms, we derive a criterion for pairing the users in NOMA which ensures the minimum required data rates are achieved for each user. We denote $\bar{R}_1$ and $\bar{R}_2$ as the minimum required data rates by the strong and weak users, respectively. Thus, both MPA and EEPA algorithms should satisfy the following constraints

$$R_1^{\text{NOMA}} \geq \bar{R}_1, \tag{13}$$
$$R_2^{\text{NOMA}} \geq \bar{R}_2. \tag{14}$$

### A. MPA

In MPA, apart from satisfying (13)-(14), we allocate the transmit powers ($\alpha_1$ and $\alpha_2$) that maximize the achievable sum rate (ASR) of the paired users, where, ASR is defined as

$$ASR = R_1^{\text{NOMA}} + R_2^{\text{NOMA}}.$$

We formulate the desired optimization as follows.

$$\max_{\alpha_1, \alpha_2} \quad R_1^{\text{NOMA}} + R_2^{\text{NOMA}}, \tag{15}$$
$$\text{s.t.} \quad (13), (14),$$
$$\alpha_1 \geq 0, \alpha_2 \geq 0, \tag{16}$$
$$\alpha_1 \leq 1, \alpha_2 \leq 1. \tag{17}$$

*1) Bounds on $\alpha_1$ and $\alpha_2$:* From (11)-(12), we get,

$$R_1^{\text{NOMA}} + R_2^{\text{NOMA}} = \log_2(1 + (\alpha_1 \gamma_1^{\text{CSI}} + \alpha_2 \gamma_2^{\text{CSI}}) \operatorname{sinc}^2(\delta)). \tag{18}$$
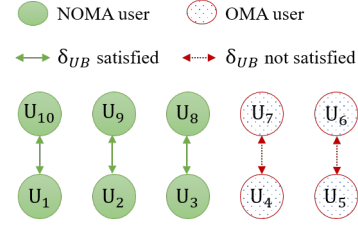


Fig. 2: Illustration of adaptive user pairing.

Thus, ASR is an increasing function with respect to $\alpha_1$ and $\alpha_2$. However, from (11), an increase in $\alpha_2$ will decrease the achievable data rate for the strong user, whereas, there is no such impact with an increase in $\alpha_1$. Hence, to maximize the ASR, we assign $\alpha_1 = 1$. Thus, we get,

$$R_1^{\text{NOMA}} = \log_2 \left( 1 + \frac{\gamma_1^{\text{CSI}} \operatorname{sinc}^2(\delta)}{1 + \alpha_2 \gamma_2^{\text{CSI}} \operatorname{sinc}^2(\delta)} \right). \tag{19}$$

From (12) and (14), we get,

$$\alpha_2 \geq \frac{2^{\bar{R}_2} - 1}{\gamma_2^{\text{CSI}} \operatorname{sinc}^2(\delta)} \triangleq \alpha_{2_{\text{LB}}}. \tag{20}$$

From (13) and (19), we get,

$$\alpha_2 \leq \frac{\gamma_1^{\text{CSI}} \operatorname{sinc}^2(\delta) + 1 - 2^{\bar{R}_1}}{\gamma_2^{\text{CSI}} \operatorname{sinc}^2(\delta)[2^{\bar{R}_1} - 1]} \triangleq \alpha_{2_{\text{UB}}}. \tag{21}$$

*2) Criterion for pairing the users:* We initially sort the users in the decreasing order of their SINRs [12]. Then, using (20)-(21), and assuming $\alpha_{2_{\text{UB}}} \geq \alpha_{2_{\text{LB}}}$, we obtain the pairing criterion for the MPA algorithm as follows.

$$\operatorname{sinc}^2(\delta) \geq \frac{2^{\bar{R}_2} \left[ 2^{\bar{R}_1} - 1 \right]}{\gamma_1^{\text{CSI}}} \triangleq \operatorname{sinc}^2(\delta_{\text{UB}}^{\text{MPA}}). \tag{22}$$

We define $\bar{R}_1$ and $\bar{R}_2$ as the achievable OMA rates, and then, pair the users in NOMA iff (22) is satisfied. Otherwise, we consider transmitting the information for the users in an OMA scenario as shown in Fig. 2. This way, the proposed algorithm ensures that a minimum of OMA rates are achieved in a worst-case scenario and it maximizes the ASR by switching to NOMA whenever feasible.

*3) Power allocation:* For the paired users, we define the power allocation factors as follows.

$$\alpha_1^{\text{MPA}} = 1, \tag{23}$$
$$\alpha_2^{\text{MPA}} = \min\{\alpha_{2_{\text{UB}}}, 1\}. \tag{24}$$

Note that in (23), the strong user transmits at maximum power to maximize the spectral efficiency, whereas, in (24), the weak user transmits at a maximum possible power that does not degrade the strong user's data rate beyond the OMA rate. Further, to avoid transmit power violations, we limit the maximum value of $\alpha_2^{\text{MPA}}$ to 1 in (24).

**Lemma 1.** *The power allocation factors formulated in* (23) - (24) *are the optimal values that achieve maximum sum rate while ensuring the individual NOMA rates to be better than the OMA counterparts.*

*Proof.* For the ease of understanding, we define

$$\eta \triangleq \frac{2^{\bar{R}_1} - 1}{\gamma_1^{\mathrm{CSI}} \mathrm{sinc}^2(\delta)}, \tag{25}$$

$$\kappa \triangleq \frac{(2^{\bar{R}_1} - 1)\gamma_2^{\mathrm{CSI}}}{\gamma_1^{\mathrm{CSI}}}. \tag{26}$$

Thus, we reformulate (15) as follows

$$\max_{\alpha_1, \alpha_2} \quad \alpha_1 \gamma_1^{\mathrm{CSI}} + \alpha_2 \gamma_2^{\mathrm{CSI}}, \tag{27}$$

$$\text{s.t.} \quad -\alpha_1 + \alpha_2 \kappa + \eta \leq 0, \tag{28}$$

$$-\alpha_2 + \alpha_{2_{\mathrm{LB}}} \leq 0, \tag{29}$$

$$\alpha_1 - 1 \leq 0, \alpha_2 - 1 \leq 0. \tag{30}$$

where, (27) is obtained by using the fact that logarithmic function is a monotonically increasing function and substituting (18) in (15). The constraint (28) is obtained by substituting (25)-(26) in (13) and the constraint (29) is obtained by further solving the (14). Additionally, since $\bar{R}_1$, $\bar{R}_2$ are non negative, we get $\alpha_{2_{\mathrm{LB}}}$, $\eta$, $\kappa > 0$, and thus, we consider the constraint (16) is already captured in (28)-(29). Next, the Lagrangian for (27) is formulated as

$$L(\alpha_1, \alpha_2, \mu_1, \mu_2, \mu_3, \mu_4) = \alpha_1 \gamma_1^{\mathrm{CSI}} + \alpha_2 \gamma_2^{\mathrm{CSI}} - \mu_1(\alpha_1 - 1)$$
$$-\mu_2(\alpha_2 - 1) - \mu_3(-\alpha_2 + \alpha_{2_{\mathrm{LB}}}) - \mu_4(-\alpha_1 + \alpha_2 \kappa + \eta).$$

Solving stationarity conditions $\frac{\partial L}{\partial \alpha_1} = 0$ and $\frac{\partial L}{\partial \alpha_2} = 0$, we get

$$\gamma_1^{\mathrm{CSI}} - \mu_1 + \mu_4 = 0, \tag{31}$$

$$\gamma_2^{\mathrm{CSI}} - \mu_2 + \mu_3 - \mu_4 \kappa = 0. \tag{32}$$

The complementary slackness conditions are formulated as

$$\mu_1(\alpha_1 - 1) = 0, \tag{33}$$

$$\mu_2(\alpha_2 - 1) = 0, \tag{34}$$

$$\mu_3(-\alpha_2 + \alpha_{2_{\mathrm{LB}}}) = 0, \tag{35}$$

$$\mu_4(-\alpha_1 + \alpha_2 \kappa + \eta) = 0. \tag{36}$$

The dual feasibility conditions are formulated as

$$\mu_i \geq 0 , \ \forall \ i \in [1, 4]. \tag{37}$$

Solving (31)-(37), we find that the possible optimal values of $(\alpha_1, \alpha_2)$ are $(\alpha_{2_{\mathrm{LB}}}\kappa + \eta, \ \alpha_{2_{\mathrm{LB}}})$, $(\kappa + \eta, 1)$, $(1, 1)$, $(1, \alpha_{2_{\mathrm{LB}}})$, and $(1, \frac{1-\eta}{\kappa})$. From (27), larger the values of $\alpha_1$ and $\alpha_2$, larger will be the ASR. Since, $\alpha_1 = 1$ has no impact on any of the desired constraints, we consider only the solutions with $\alpha_1 = 1$ which are $(1, 1), (1, \alpha_{2_{\mathrm{LB}}})$, and $(1, \frac{1-\eta}{\kappa})$. Note that considering $(\alpha_1, \alpha_2) = (1, 1)$ will violate the constraint (28). Hence, by substituting $\alpha_{2_{\mathrm{UB}}} = \frac{1-\eta}{\kappa}$, the optimal values of $(\alpha_1, \alpha_2)$ are either $(1, \alpha_{2_{\mathrm{UB}}})$ or $(1, \alpha_{2_{\mathrm{LB}}})$. Since, $\alpha_{2_{\mathrm{UB}}} \geq \alpha_{2_{\mathrm{LB}}}$, we conclude $(\alpha_1, \alpha_2) = (1, \alpha_{2_{\mathrm{UB}}})$ as the optimal solution. This completes the proof of the Lemma 1. ∎

Next, we present the EEPA algorithm.

### B. EEPA

In EEPA, apart from satisfying (13)-(14), we allocate the powers ($\alpha_1$ and $\alpha_2$) that maximize the energy efficiency (EE) of the paired users, where, EE is defined as

---

**Algorithm 1:** Proposed algorithms

**Inputs** : $\gamma_i^{\mathrm{CSI}}$, $\forall i \in [1, G]$.
**Variables:** $i$ represents the user pairing index.

1 Sort the $G$ users in decreasing order of $\gamma_i^{\mathrm{CSI}}$;
2 Set $i = 1$;
3 **while** $i < \frac{G}{2} + 1$ **do**
4 $\quad$ Consider $i^{th}$ user as strong user and $(G - i + 1)^{th}$ user as the weak user;
5 $\quad$ Calculate $\bar{R}_1$, $\bar{R}_2$ from (10);
6 $\quad$ **if** *MPA* **then**
7 $\quad\quad$ Calculate $\delta_{\mathrm{UB}}^{\mathrm{MPA}}$ from (22);
8 $\quad\quad$ **if** $\delta \leq \delta_{UB}^{MPA}$ **then**
9 $\quad\quad\quad$ Pair the users in NOMA with $\alpha_1=1$, $\alpha_2=\min\{\alpha_{2_{\mathrm{UB}}}, 1\}$ as per (23), (24)
10 $\quad\quad$ **else**
11 $\quad\quad\quad$ Consider the users in OMA;
12 $\quad\quad$ **end**
13 $\quad$ **else if** *EEPA* **then**
14 $\quad\quad$ Calculate $\delta_{\mathrm{UB}}^{\mathrm{EEPA}} = \min\{\delta_{\mathrm{UB}_1}, \delta_{\mathrm{UB}_2}\}$ from (40);
15 $\quad\quad$ **if** $\delta \leq \delta_{UB}^{EEPA}$ **then**
16 $\quad\quad\quad$ Pair the users in NOMA with $(\alpha_1, \alpha_2)$ obtained from the solution of (38);
17 $\quad\quad$ **else**
18 $\quad\quad\quad$ Consider the users in OMA;
19 $\quad\quad$ **end**
20 $\quad$ $i = i + 1$;
21 **end**

---

$$EE = \frac{ASR}{\alpha_1 + \alpha_2},$$
$$= \frac{\log_2\left[1 + \left(\alpha_1 \gamma_1^{\mathrm{CSI}} + \alpha_2 \gamma_2^{\mathrm{CSI}}\right) \mathrm{sinc}^2(\delta)\right]}{\alpha_1 + \alpha_2}.$$

Thus, we formulate the optimisation problem as follows.

$$\max_{\alpha_1, \alpha_2} \quad \frac{\log_2\left[1 + \left(\alpha_1 \gamma_1^{\mathrm{CSI}} + \alpha_2 \gamma_2^{\mathrm{CSI}}\right) \mathrm{sinc}^2(\delta)\right]}{\alpha_1 + \alpha_2}, \tag{38}$$

$$\text{s.t.} \quad (28) - (30).$$

*1) Criterion for pairing the users:* Solving (28) for a worst case scenario of $\alpha_2 = 1$, we get,

$$\alpha_1 \geq \kappa + \eta = \frac{2^{\bar{R}_1} - 1}{\gamma_1^{\mathrm{CSI}}}\left[\gamma_2^{\mathrm{CSI}} + \frac{1}{\mathrm{sinc}^2(\delta)}\right]. \tag{39}$$

Using (39) in (17), we get,

$$\frac{2^{\bar{R}_1} - 1}{\gamma_1^{\mathrm{CSI}}}\left[\gamma_2^{\mathrm{CSI}} + \frac{1}{\mathrm{sinc}^2(\delta)}\right] \leq 1,$$

$$\mathrm{sinc}^2(\delta) \geq \frac{1}{\left(\frac{\gamma_1^{\mathrm{CSI}}}{2^{\bar{R}_1} - 1}\right) - \gamma_2^{\mathrm{CSI}}} \triangleq \mathrm{sinc}^2(\delta_{\mathrm{UB}_1}).$$

Using (20) in (17), we get,

$$\alpha_{2_{\mathrm{LB}}} \leq 1,$$

$$\mathrm{sinc}^2(\delta) \geq \frac{2^{\bar{R}_2} - 1}{\gamma_2^{\mathrm{CSI}}} \triangleq \mathrm{sinc}^2(\delta_{\mathrm{UB}_2}).$$

(a) $\gamma_1^{\text{CSI}}, \gamma_2^{\text{CSI}} = [8,5]$ dB, $\delta=0°$.    (b) $\gamma_1^{\text{CSI}}, \gamma_2^{\text{CSI}} = [8,5]$ dB, $\delta=11°$.    (c) $\gamma_1^{\text{CSI}}, \gamma_2^{\text{CSI}} = [8,2]$ dB, $\delta=0°$.    (d) $\gamma_1^{\text{CSI}}, \gamma_2^{\text{CSI}} = [8,2]$ dB, $\delta=11°$.
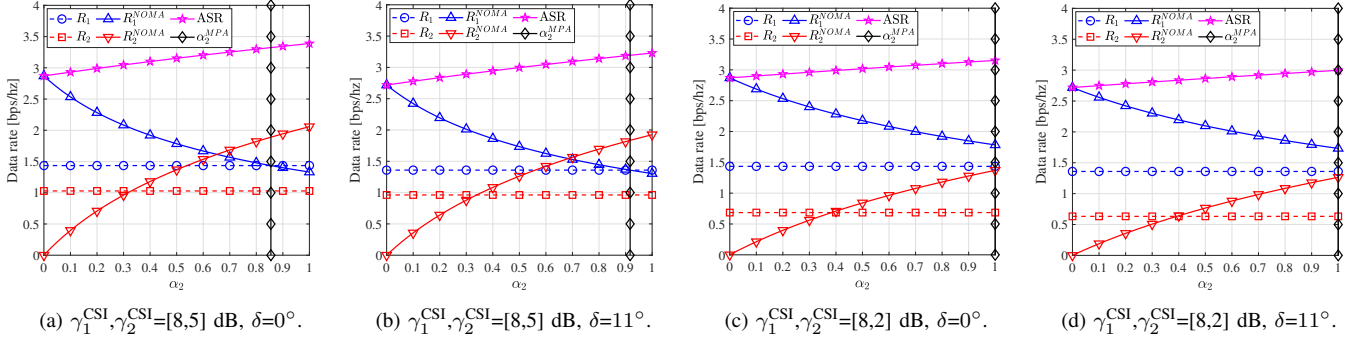
Fig. 3: Comparison of achievable data rates for varying power allocation factor of the weak user.



(a) $\gamma_1^{\text{CSI}}, \gamma_2^{\text{CSI}} = [8,5]$ dB.    (b) $\gamma_1^{\text{CSI}}, \gamma_2^{\text{CSI}} = [8,2]$ dB.     (a) Mean $R_1$ vs $\delta$.     (b) Mean $R_2$ vs $\delta$.
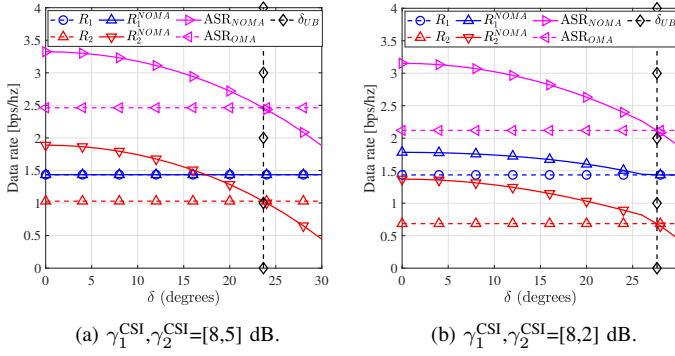
Fig. 4: Comparison of achievable data rates for varying imperfection in phase.

Fig. 5: Comparison of mean achievable data rates of strong and weak user with various algorithms.

Thus, we define the upper bound on the phase imperfection in EEPA as

$$\delta_{\text{UB}}^{\text{EEPA}} = \min\{\delta_{\text{UB}_1}, \delta_{\text{UB}_2}\}. \tag{40}$$

We define $\bar{R}_1$ and $\bar{R}_2$ as the achievable OMA rates, and then, pair the users in NOMA iff the imperfection in the phase compensation is less than $\delta_{\text{UB}}^{\text{EEPA}}$. Otherwise, we consider transmitting the information for the users in an OMA scenario as shown in Fig. 2.

*2) Power allocation:* The objective function formulated in (38) is a strictly pseudo-concave function [13] and an efficient way of obtaining a solution is to use the Dinkelbach's algorithm [13], [14]. An outline of implementing MPA and EEPA is presented in detail in Algorithm 1.

## IV. NUMERICAL RESULTS

For the simulations, we have considered $M = 8$, $N = 32$, and $\bar{R}_i = R_i^{\text{OMA}}$. We have then dropped the BSs and users from Poisson point distribution with densities of 25 BS/km$^2$ and 2000 users/km$^2$, respectively. For each user, we have calculated the path loss and the received signal power from each BS by considering the urban cellular path loss model presented in [15]. The users are then associated to the BS from which they receive the maximum signal power, and the rest of the BSs are considered as interfering BSs. Given this simulation set-up, we have calculated various performance metrics with the proposed and the existing state-of-the-art algorithms which are summarised as follows.

In Fig. 3, we present the achievable data rates for varying $\alpha_2^{\text{MPA}}$. For the evaluation, we consider two configurations of
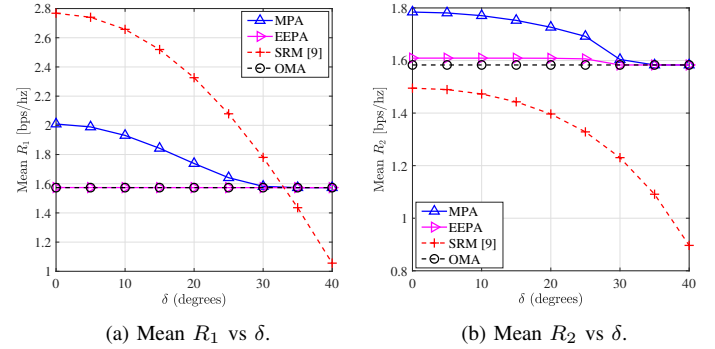
user pairs with $[\gamma_1^{\text{CSI}}, \gamma_2^{\text{CSI}}] = [8, 5]$ dB, $[\gamma_1^{\text{CSI}}, \gamma_2^{\text{CSI}}] = [8, 2]$ dB, and two configurations of imperfection in phase compensation, $\delta = 0°, 11°$. As shown in Fig. 3, with increasing $\alpha_2$, the data rates for weak user increases. This increase in $\alpha_2$ also increases interference for the strong user, and thus, the achievable data rate for the strong user decreases. Note that for a fixed $\delta$, the achievable data rates and sum rate are better in Fig. 3a as compared to Fig. 3c because of the better SINR conditions. Further, with an increase in the $\delta$, the achievable data rates and sum rate are smaller in Fig. 3b when compared to Fig. 3a. As shown in Fig. 3, the ASR is a non-decreasing function of $\alpha_2$ which aligns with our formulation in the Section III-A. Further, beyond the proposed $\alpha_2 = \alpha_2^{\text{MPA}}$, the individual data rates are not better than the OMA counterparts. Thus, we validate the proposed bounds on power allocation factors in the presence of imperfect phase compensation.

In Fig. 4, we present the comparison of the achievable data rates for varying $\delta$. For the evaluation, we consider two configurations of user pairs with $[\gamma_1^{\text{CSI}}, \gamma_2^{\text{CSI}}] = [8, 5]$ dB and $[\gamma_1^{\text{CSI}}, \gamma_2^{\text{CSI}}] = [8, 2]$ dB in Fig. 4a and Fig. 4b, respectively. Further, we consider $\alpha_1 = 1$ and $\alpha_2 = \alpha_2^{\text{MPA}}$ while calculating the achievable data rates. With an increase in $\delta$, the achievable rates decrease. Additionally, whenever $\delta < \delta_{\text{UB}}^{\text{MPA}}$, the achievable data rates and sum-rates are always better than the OMA counterparts. Thus, we validate the proposed bound on the imperfection in the phase compensation. Note that a similar analysis is extendable for the EEPA scenario.

In Fig. 5, we present the performance comparison of mean of achievable data rates with various algorithms. As shown in
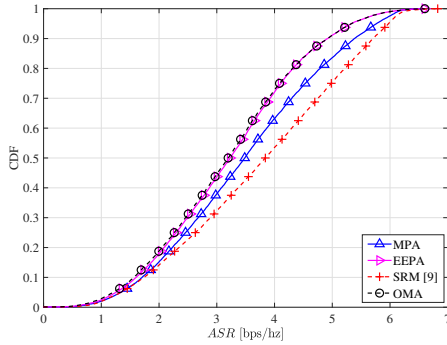
Fig. 6: Comparison of mean of achievable data rates of strong and weak user with various algorithms.



(a) Mean ASR vs $\delta$.  (b) Mean EE vs $\delta$.

Fig. 7: Comparison of mean achievable sum rate and energy efficiency with various algorithms.

Fig. 5, for both strong and weak user, the performance of sum rate maximisation (SRM) [9] declines gradually with increase in $\delta$ and the data rates fall below OMA for larger $\delta$. In case of the proposed algorithms, both MPA and EEPA consider the imperfections in the phase compensation, and hence, the data rates gradually converge to OMA the rates with an increase in $\delta$. Further, as shown in Fig. 5b, the SRM algorithm tries to maximize the ASR and in the process significantly decreases the weak user data rates beyond the required OMA rates. However, the MPA algorithm maximizes the strong user rate to achieve maximum ASR and yet ensures both strong and weak user achieve minimum of OMA rates. The EEPA algorithm allocates minimum power to each user to ensure the minimum required OMA rates are achieved, and hence, the data rates with EEPA are significantly lower than MPA rates and slightly higher than the OMA rates.

In Fig. 6, we present the comparison of the mean ASR with the proposed algorithms against the SRM and OMA in the presence of imperfect phase compensation. As shown in Fig. 6, SRM achieves highest ASR as compared to all the algorithms. However, as shown in Fig. 5, the SRM does not achieve minimum required rates for the weak user, whereas, the proposed MPA maximizes ASR while ensuring a minimum of OMA rates for both strong and weak users. Further, note that with EEPA, the achievable sum rate is slightly higher than the OMA rates.

In Fig. 7, we present the comparison of the mean achievable sum rate and energy efficiency with various algorithms. As shown in Fig. 7a and 7b, the SRM has highest mean ASR and EE at the lower $\delta$. However, note that SRM algorithm does not ensure that individual users achieve a minimum of OMA rates. Further, with increasing $\delta$, the mean ASR and EE of the both the proposed algorithms converge to the OMA rates, whereas, the performance of the SRM degrades significantly as compared to the OMA rates. Hence, it is not always beneficial to pair the users in NOMA. Thus, we conclude that, the proposed algorithms outperform the existing algorithms in presence of imperfection in phase compensation. Additionally, they also maximize the data rates or energy efficiency while ensuring minimum required data rates for each user.
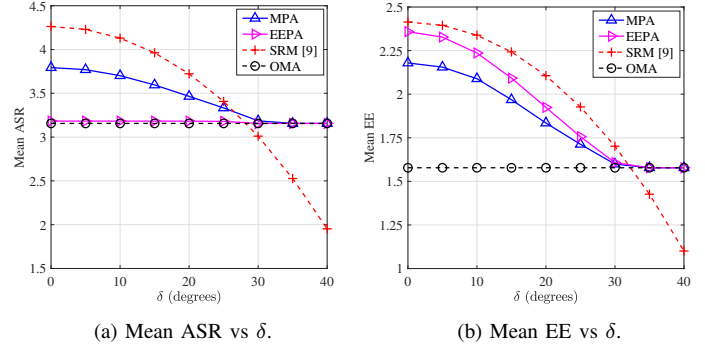
## V. CONCLUSION

We have proposed adaptive user pairing algorithms for RIS-assisted uplink NOMA systems that maximize the achievable sum-rate or energy efficiency. We have formulated the criterion for user pairing based on the derived bounds on imperfection in the phase compensation. Through numerical results, we have validated the derived bounds and the proposed pairing criterion. Further, we have proposed novel power allocation procedures for the paired users. We have performed extensive system-level simulations and have shown that the proposed algorithms achieve significant improvement over the state-of-the-art algorithms with increase in phase imperfection. In the future, we plan to validate the proposed algorithms on the hardware test-beds.

## REFERENCES

[1] A. Kassir *et al.*, "Power Domain Non Orthogonal Multiple Access: A Review," in *Proc. TAFGEN*, 2018, pp. 66–71.

[2] 3GPP, "Study on Non-Orthogonal Multiple Access (NOMA) for NR," Technical Report 38.812, v 16.0.0, Dec. 2018.

[3] M. S. Ali *et al.*, "Dynamic User Clustering and Power Allocation for Uplink and Downlink Non-Orthogonal Multiple Access (NOMA) Systems," *IEEE Access*, vol. 4, pp. 6325–6343, 2016.

[4] Z. Ding and H. V Poor, "A Simple Design of IRS-NOMA Transmission," *IEEE Commun. Lett.*, vol. 24, no. 5, pp. 1119–1123, 2020.

[5] J.-C. Chen, "Machine Learning-Inspired Algorithmic Framework for Intelligent Reflecting Surface-Assisted Wireless Systems," *IEEE Trans. on Veh. Technol.*, pp. 1–1, 2021.

[6] Pavan Reddy M. and A. Kumar, "User Pairing and Power Allocation for IRS-Assisted NOMA Systems with Imperfect Phase Compensation," *arXiv*, cs.IT 2106.07938, 2021.

[7] S. Xia and Y. Shi, "Intelligent Reflecting Surface for Massive Device Connectivity: Joint Activity Detection and Channel Estimation," in *Proc. IEEE ICASSP*, 2020, pp. 5175–5179.

[8] Z. Wang *et al.*, "Channel Estimation for IRS-Assisted Multiuser Communications," in *Proc. IEEE WCNC*, 2020, pp. 1–6.

[9] M. Zeng *et al.*, "Sum Rate Maximization for IRS-Assisted Uplink NOMA," *IEEE Commun. Lett.*, vol. 25, no. 1, p. 234–238, Jan 2021.

[10] G. Yang *et al.*, "Intelligent Reflecting Surface Assisted Non-Orthogonal Multiple Access," in *Proc. IEEE WCNC*, 2020, pp. 1–6.

[11] S. Zhou *et al.*, "Spectral and Energy Efficiency of IRS-Assisted MISO Communication With Hardware Impairments," *IEEE Wireless Commun. Lett.*, vol. 9, no. 9, pp. 1366–1369, 2020.

[12] N. S. Mouni *et al.*, "Adaptive User Pairing for NOMA Systems With Imperfect SIC," *IEEE Wireless Commun. Lett.*, vol. 10, no. 7, pp. 1547–1551, 2021.

[13] A. Zappone *et al.*, "Energy Efficiency in Secure Multi-Antenna Systems," *arXiv*, cs.IT 1505.02385, 2015.

[14] M. Zeng *et al.*, "Energy-Efficient Power Allocation for Uplink NOMA," in *Proc. IEEE GLOBECOM*, 2018, pp. 1–6.

[15] 3GPP, "Study on channel model for frequencies from 0.5 to 100 GHz,," Technical Report 38.901, v 16.0.0, Jan. 2020.